Ion channels as biomarkers of altered myogenesis in myofiber precursors of Duchenne muscular dystrophy

Alessandro Giovanni Cerchiara[1*], Paola Imbrici[1*], Raffaella Quarta[1], Enrica Cristiano[1], Brigida Boccanegra[1], Erika Caputo[1], Dominic J. Wells [2], Ornella Cappellari[1], Annamaria De Luca[1]

[1]Department of Pharmacy – Drug Sciences, University of Bari Aldo Moro, Bari, Italy

[2]Department of Comparative Biomedical Sciences, The Royal Veterinary College, London, UK

*Contributed equally to this work and share first authorship

Correspondences

Ornella Cappellari and Annamaria De Luca

Department of Pharmacy – Drug Sciences

University of Bari Aldo Moro,

Via Orabona 4

Bari, Italy 70125

Graphical abstract

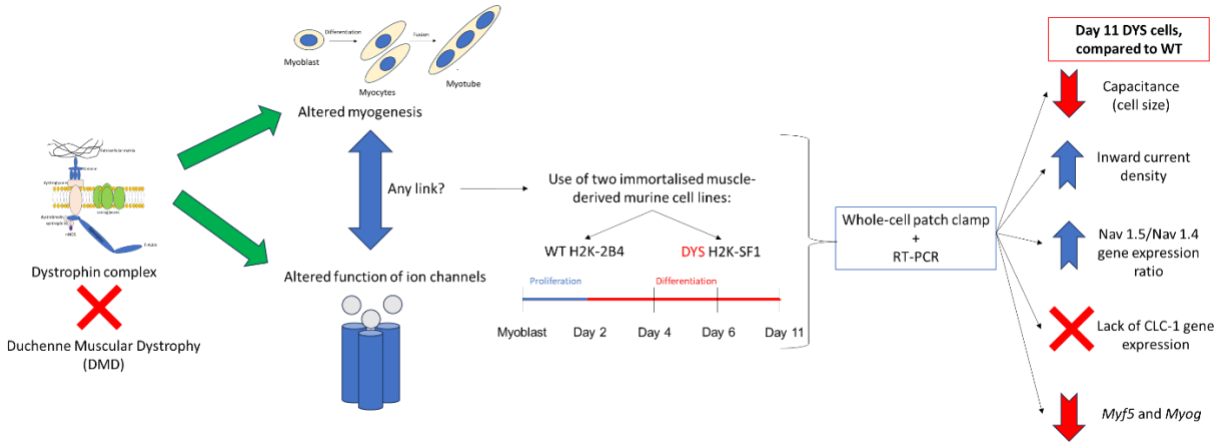

Ion channels have an active crosstalk with the dystrophin complex, which is disrupted in Duchenne muscular dystrophy, but little is known about their involvement in myogenesis, especially in dystrophic settings. We performed an electrophysiological characterization of wild-type and dystrophic myoblasts/myocytes to shed light on the relationship between dystrophin loss and ion channel activity during myogenesis with the final aim to identify new biomarkers and drug targets in regenerative medicine approaches.

Abstract

Myogenesis is essential for skeletal muscle formation, growth, and regeneration and can be altered in Duchenne muscular dystrophy (DMD), an X-linked disorder due to the absence of the cytoskeletal protein dystrophin. Ion channels play a pivotal role in muscle differentiation and interact with the dystrophin complex. To investigate ion channels involvement in myogenesis in dystrophic settings, we performed an electrophysiological characterization at day 0, 2, 4, 6, and 11 in two immortalized mouse cell lines: the wild-type H2K-2B4 (WT) and the dystrophic H2K-SF1 (DYS). Moreover, we measured gene expression of differentiation markers and ion channels. Inward and outward currents/density increased as the differentiation progressed both in WT and DYS cells. However, day-11 DYS cells showed higher (27%) inward current density with increased expression ratio of SCN5A/SCN4A, and decreased (48%) and less barium-sensitive outward current, compared to WT. Furthermore, day-11 DYS cells showed more positive resting membrane potential (+10mV) and lower membrane capacitance (50%), compared to WT. DYS cells also presented reduced *Myog* and *MYF5* expression at day 6 and 11. Overall, ion channel profile and myogenesis appear altered in DYS cells. This first step paves the way to validate ion channels as potential drug targets to ameliorate muscle degeneration in DMD settings and as differentiation biomarkers in innovative platforms.

INTRODUCTION

Myogenesis is essential for skeletal muscle formation, growth, and regeneration. This process normally happens during muscle formation in embryogenesis and during muscle regeneration in

adults. During embryogenesis, skeletal muscle formation is a step-wise process that derives from somites and classes of myogenic-committed progenitor satellite cells [1,2]. Satellite cells play a key role in increasing muscle fiber size since, after division, a percentage of the progenitor cells fuse with the nearby fiber to form bigger multinucleated myofibers. After skeletal muscle formation and post-natal growth, satellite cells became quiescent and are activated when the muscle is damaged. In muscle repair process, satellite cell activation leads to their proliferation and differentiation to form a new fiber; in parallel, proliferation allows repopulating of the residual pool of stem cells, ensuring repairing ability in case of a new muscle injury [3].

The deep understanding of the mechanisms underlying intrinsic myogenesis is crucial to identify novel druggable targets to drive effective regeneration processes in degenerative neuromuscular conditions. Moreover, it could also be useful to build up and monitor proper development of muscle organoids to be used as disease models and innovative experimental platforms for regenerative medicine purposes [4,5].

Emerging yet contrasting evidence suggests that muscle satellite cells and myogenesis can be altered in inherited muscle disorders such as Duchenne muscular dystrophy (DMD), an X-linked disorder due to defects in the dystrophin gene which lead to the absence of the cytoskeletal protein dystrophin. Dystrophin has a clear role in differentiated myofibers where it confers stability and contributes to mechano-transduction via the interaction with dystrophin–glycoprotein complex (DGC), extracellular matrix components, and various cytolinkers involved in intracellular signaling, metabolism, and homeostasis [6,7]. When dystrophin protein expression is reduced (Becker Muscular dystrophy) or totally absent (DMD), the stability of the membrane is not maintained and tears and/or abnormal activation of mechanosensitive-channels lead to increased calcium influx in DMD myotubes [8] and fibers [9]. The consequences of both dystrophin absence and DGC disassembling appear post-natally during the full acquisition of motor skills, with impairment of force transduction and progressive muscle weakness and damage, followed by chronic inflammation and inefficient

regeneration [10,11]. While inefficient regeneration is believed to be a main consequence of the hostile inflammatory and pro-fibrotic environment—as well as satellite cell exhaustion due to continuous regeneration cycles—intrinsic defects of satellite cells have been proposed as a key process leading to defective cell division, reduced myogenic commitment and delayed differentiation [12,13]. All these features can contribute to disease progression via an impaired regenerative potential. Interestingly, dystrophin expression has been detected in satellite cells, supporting the early role of this protein in satellite cell polarization and commitment [14].

Ion channels can be important, yet poorly explored, players in myogenesis due to their involvement in both key housekeeping processes and highly specialized cell and tissue functions. Ion channels are transmembrane ion selective paths that allow rapid biophysical events in response to voltage, mechanical, or chemical signals thus controlling a plethora of functions in tissues. In fact, in differentiated skeletal muscle, ion channels are pivotal for maintaining the resting membrane potential (RMP), priming excitation–contraction coupling, and regulating calcium homeostasis. [15,16] Accordingly, the proper expression of ion channels can play a role in different myogenesis-related processes, such as fusion and myotube formation as well as self-renewal of satellite cells [17–19,]. For instance, in fusion-competent myoblasts, Kir2.1 expression is pivotal for the hyperpolarization of the resting membrane potential that is required to induce early fusion of two myocytes [17,18].

However, the precise role of ion channels in early myogenesis and their potential as either biomarkers and/or drug targets in regeneration remains elusive. Even less clear is the relationship between the pattern of ion channel development and the proposed defective myogenesis of dystrophic satellite cells. This is of interest considering that dystrophin and its linkers (i.e., α-syntrophin) interact with several ion channels—in line with the proposed role of DGC in providing structural scaffold for the positioning of ion channels and other proteins at the sarcolemma in skeletal muscle [21]. Particularly in differentiated myofibers, DGC can interact with different sodium

($Na_v1.4$ and $Na_v1.5$)[22], calcium ($Ca_v1.1$, TRPC1, and TRPC4) [23,24], and potassium channels (Kir2.1) [25] as well as with the water channel aquaporin 4 [26].

In order to gain insight into the efficiency of the myogenic program in DMD and the contribution of ion channels to myogenesis, we performed an electrophysiological characterization of the total outward and inward currents that are important for setting the RMP and excitability properties in two immortalized mouse satellite-derived myoblasts at different time points of differentiation. The wild-type H2K-2B4 (WT) and the dystrophic H2K-SF1 (DYS)[27,28] myoblasts retain myogenic capability under specific culture conditions. In parallel, we utilized RT-PCR to analyze the gene expression profile of the main markers of differentiation and ion channels that possibly account for the outward and inward currents throughout the different stages of differentiation.

Our data show that during myogenesis intrinsic impairments in ion channel development may in fact occur in the dystrophic condition, likely in relation to the primary defect. This reinforces our long-term objective to gain more insight into the contribution of specific ion channels to the myogenic program that could be useful to ameliorate muscle regeneration through pharmacological modulation and determine functional biomarkers in muscle organoids.

MATERIALS AND METHDOS

Cell cultures

We used the immortalized myoblast-derived cell line (H2K-2B4) and its immortalized dystrophic counterpart (H2K-SF1) developed from healthy and *mdx* mice by Muses et al. as previously

described [27–29]. 2B4 and SF1 cells were cultured in both proliferative (myoblasts) and differentiation (myocytes/myotubes) medium. Myoblasts were cultured in growth medium composed of the following: DMEM high glucose with sodium pyruvate (Immunological Sciences), 20% (v/v) heat inactivated-fetal bovine serum (Immunological Sciences), 2% (v/v) chicken embryo extract (Thermo Fisher Scientific), 4 mM L-glutamine (Immunological Sciences), and 1% (v/v) penicillin/streptomycin (Immunological Sciences). We coated wells with 0.1 mg/ml of Cultrex® 3-D Culture Matrix RGF Basement Membrane Extract or Matrigel (Bio-techne®) to encourage cell adhesion and incubated them for 40 minutes at 33°C before removing any Matrigel excess. Each cell line contains a thermolabile t-Antigen protein that maintains cells at the proliferative state. In order to initiate its expression, we added 20 U/mL of interferon gamma (IFN-γ; Sigma-Aldrich®) to the growth medium, and we cultured 2B4/SF1 cells at 33°C with 5% CO_2.

To trigger terminal differentiation, we cultured 2B4 and SF1 cells in differentiation medium composed by DMEM, 5% (v/v) horse serum (Sigma-Aldrich®), 4 mM L-glutamine, and 1% penicillin/streptomycin (Immunological Sciences). Plates were coated with Matrigel as described above. Cells were cultured at 37°C with 5% CO2 without IFN- γ. We differentiated cell lines for 2, 4, 6, and 11 days, changing half of the differentiation medium every two days. Seeding density was set at 2.5×10^4 cells for both proliferation and differentiation conditions. For clarity, 2B4 cells will be indicated as WT cells and SF1 cells as DYS cells throughout the paper.

The bright-field images of WT and DYS myoblasts and myotubes (D11) at 10X magnification were taken with CL-I Eclipse microscope (Nikon).

Electrophysiological recordings

Inward and outward currents were evaluated at different time points of proliferation and differentiation. Besides the proliferative state (myoblasts; Day 0), four additional time points of differentiation were observed: the 2nd (D2), the 4th (D4), the 6th (D6), and the 11th day (D11) for

each cell line. For patch clamp measurements we selected fused cells, which presented with spindles and an elongated form with Cm < 100pF.

Whole cell patch clamp recordings of inward and outward currents were performed using an Axopatch 1D amplifier and Digidata 1440A analog-digital converter (Molecular Devices, San Jose, CA, USA). Experiments were carried out at room temperature (~22 °C). Patch pipettes were pulled using a vertical micropipette puller (Narishige, Tokyo, Japan) and electrodes had a resistance of 4–6 MΩ. Current acquisition and data analysis were performed using the pCLAMP 10.6 and Clampfit software (Molecular Devices, San Jose, CA, USA). Current signals were filtered at 5 kHz and sampled at 10 kHz. Leak currents were always <200 pA at the holding potential (-80 mV). Only cells with access resistance <10 MΩ were used.

The extracellular solution contained 130 mM NaCl, 3 mM KCl, 1 mM $CaCl_2$, 2 mM $MgCl_2$, 10 mM HEPES-HCl, and 10 mM glucose (pH 7.4), and the patch pipette was filled with an intracellular solution containing 130 mM KCl, 2 mM $MgCl_2$, 5 mM EGTA, 10 mM HEPES-NaOH, and 10 mM glucose (pH 7.4) [30].

Five µM of tetrodotoxin (Abcam) and 500 µM $BaCl_2$ (Sigma-Aldrich Merck Life Science, Milano, Italy) were used as tools to better identify the contribution of Na_v and Kir channels to the recorded currents, respectively [31], and were dissolved in the extracellular solution and added to the Petri dish after performing a control recording. As we could not predict the kind and amount of inward and outward currents in both conditions and during differentiation at the time of recording, we used standard protocols to detect any type of current. We maintained the same voltage protocol throughout all experiments

To determine the current–voltage relationships, cells were clamped to a holding potential of -80 mV and currents were elicited with 250 ms pulses from -100 mV to +70 mV, with a ΔV of 10 mV (5-s inter-pulse duration). To compare currents in different cells, we measured the peak inward

current at -20mV and steady-state outward current at + 60mV. In our analysis, we also included cells that presented with either inward or outward currents. Membrane capacitance (Cm) was assessed in whole-cell configuration and before starting the protocol. The RMP was measured in zero-current mode of current clamp in whole-cell configuration before starting the voltage clamp protocol. The total inward and outward current was normalized to the Cm to obtain current density (pA/pF).

RNA extraction, reverse transcription, and gene expression

Gene expression experiments were performed at the myoblast stage and the various differentiation time points (as discussed above). RNA was extracted with the RNeasy Micro kit (QIAGEN©) following the supplier's instructions[32]. Variable amounts of RNA (between 1–2 µg) were then retro-transcribed to cDNA with iScript gDNA Clear cDNA Synthesis Kit (172-5035 Bio-Rad Laboratories, Inc, CA, USA) following manufacturer instructions. qRT-PCR was performed via the CFX384 Connect Real-Time PCR System (Bio-Rad, Hercules, CA, USA) by using PrimePCR assays SYBR® green with custom made plates. For each experiment, samples were analyzed with technical duplicates. The mRNA expression of genes was normalized to the mean of two housekeeping genes, *Actb* and *Hprt*, and quantified by the $2^{\Delta\Delta ct}$ method. Primers were purchased with the following Unique Assay IDs (Table 1).

Immunofluorescence

WT and DYS cells were grown on plates at seeding density of 2.5×10^4 for 11 days. Cells were fixed in PFA for 10 min at room temperature (RT) and permeabilized with 0.1% TWEEN (Sigma-Aldrich Merck Life Science, Milano, Italy) in 0.1% bovine serum albumin (BSA; Sigma-Aldrich

Merck Life Science, Milano, Italy) and PBS for 45 min at RT. After washes with PBS, cells were blocked in saturation buffer (0.1% BSA in PBS) and incubated with rabbit polyclonal anti- $Na_v1.4$ (1:100; ASC-020; Alomone Labs, Jerusalem, Israel) and anti-$Na_v1.5$ (1:200; ASC-005; Alomone Labs, Jerusalem, Israel) primary antibodies and anti-myosin primary antibody (MF-20-S; 1:10; Developmental Studies Hybridoma Bank, Iowa, USA), rabbit polyclonal anti-Kir2.1 antibody (1:200; APC-026; Alomone Labs, Jerusalem, Israel), anti-dystrophin (rod-domain) primary antibody, (DYS1-CE; 1:500; Leica Biosystems) and Alexa Fluor™ 488 Phalloidin (A12379; 1:400; Invitrogen™) for 1 h at RT in blocking buffer. After three washes in PBS, cells were incubated with 488/594 Alexafluor-conjugated secondary antibodies (1:1000; ThermoFisher Scientific, Waltham, MA, USA) for 1 h at RT. Nuclei staining was assessed with PureBlu™ Hoechst 33342 Nuclear staining Dye (1:50; Bio-Rad, Hercules, CA, USA). Images were captured using a dark-field microscope (CL-I Eclipse Nikon) at 20X magnification.

Statistics

Data analysis was performed using Graphpad 8.4.3. (Prism) and CFX Maestro 2.3 (Bio-Rad). All data are shown as the mean ± standard error of the Mean (S.E.M.). Statistical differences between two groups of data sets at the same point from two different cell lines (WT vs DYS) were assessed by two-tailed unpaired Student's t test and considered significant if $p<0.05$. Detailed statistical values are listed in Supporting Table S1. Statistical differences among data sets throughout differentiation (e.g., current density) within a group (WT or DYS) were assessed by using a one-way ANOVA and considered significant if $p <0.05$. Detailed statistical values are listed in Supporting Table S2.

RESULTS

Differentiation profile of WT and DYS myoblasts/myocytes

For this study we used an immortalized myoblast-derived cell line (WT) and its dystrophic counterpart (DYS) in proliferation (D0) and at different time points of differentiation (D2–D11; Figure 1 for D0 and D11). In order to first gain insight into the efficiency of the myogenic program in DMD, we evaluated the gene expression of *Myf5*, (a marker of myogenic commitment), as well as myogenin (*Myog*) and dystrophin (*Dmd*) (two markers of late differentiation) [33] in WT and DYS cells from D0 to D11(Figure 2).

Myf5 expression reached its peak at D6 and then decreased at D11 in WT cells. The expression of *Myf5*was significantly downregulated at all time points in DYS cells compared to control (Figure 2A; Supporting Table S1). We did not find any expression of *Myf5* in DYS cells at D2 and D4. As expected, *Myog* expression was low until D4, and it reached its peak at D11 in WT cells. *Myog* expression was reduced in DYS cells at D6 and D11, compared to WT (Figure 2B;Supporting Table S1). Finally, *Dmd* expression was present only at D11 in WT cells, whereas it was found to be expressed at D0, D4, and D6 and overexpressed at D11 in DYS cells (Figure 2C; Supporting Table S1), compared to control, but immunofluorescence data did not show the presence of the dystrophin protein in DYS cells (Figure 2D). This apparent contradictory data, has been observed by other authors [34], and might be related to a compensatory mechanism to a failing translation process of mutant transcript in DYS cells during differentiation.

The expression of *Myog* and *Myf5* at D11 confirmed the maturation of WT cells. Moreover, since dystrophin (a marker of late differentiation) was expressed in WT cells after 11 days of differentiation, we considered that D11 could be sufficient to contain matured myotubes.

Membrane capacitance and resting membrane potential in WT and DYS myoblasts/myocytes

To study the relationship between myogenesis and membrane electrophysiological properties as well as the potential effect of a dystrophic background, we first measured Cm and RMP of WT and DYS myoblasts (D0) and myocytes at different time points of differentiation (D2–D11).

It is generally assumed that Cm is proportional to the cell surface area and results from the membrane composition of the phospholipid bilayer [35]. To verify whether differences in the Cm exist in WT and DYS myocytes, we compared the average Cm of both cell types at different time points. Cm increased as the differentiation program progressed in both cell lines (Figures 3A and B). However, D11 DYS cells showed significantly lower Cm compared with D11 WT myocytes (Figure 3A; Table 2; Supporting Table S1), suggesting a reduced cell size and/or modified membrane composition.

We also assessed the RMP of WT and DYS cells at the different time points, as an indirect index of cell differentiation. Previous studies showed that myoblasts show less negative RMP whereas differentiated skeletal muscle cells have more negative RMP due to the higher expression of potassium channels [30,36–38]. In fact, as Figure 2B shows, D0 WT/DYS myoblasts present a depolarized RMP, which was consistent with the barely detectable outward currents (see next section). RMP became more negative as the differentiation progressed in both cell lines. However, D11 DYS cells showed a more depolarized RMP compared with D11 WT cells, albeit not statistically significant (Figure 3B; Table 2; Supporting Table S1).

Inward and outward current density in WT and DYS myoblasts/myocytes

To determine possible differences in the ion channel profiles of WT and DYS cells, we analyzed inward and outward current density from WT and DYS myoblasts (D0) and myocytes (D2–D11) at the same time points of differentiation (Figure 4 and 5). At D0, most cells were found to be without recordable current both in WT (seven out of 11) and in DYS (seven out of 10) groups. Even when detectable, both WT and DYS myoblasts showed much lower inward and outward currents, compared to differentiated WT/DYS myocytes (Figure 4A, B and 5A, B). Conversely, from D2 to D11, the number of cells without measurable currents progressively decreased and, in parallel, both inward and outward currents increased. At D6 and D11, inward and outward currents were clearly detectable in both cell lines despite showing high variability in amplitude. As shown in the insets and IV curves of Figure 4A and B, at D11 inward currents activate at about -70 mV, peak at about -40 mV and decrease in amplitude at more depolarized potentials due to a reduction in driving force whereas slowly activating and non-inactivating outward currents increase with membrane depolarization.

As shown in the IV relationships in Figure 4A–C obtained during measuring peak inward currents, WT cells inward current densities increased up to D6 and slightly declined at D11 whereas DYS cells inward current densities increased up to D11 (Figure 4A-C; Table 2). The comparison between WT and DYS cells revealed that D11 DYS cells had slightly higher inward current density (~ 27%), albeit not significantly compared with WT (at -20mV; Figure 4B; Table 2; Supporting Table S1).

Five µM tetrodotoxin (TTX) remarkably blocked inward current density at D11 by 98% and 87% in WT and DYS, respectively (Figure 4D; Table 2), supporting the potential predominant involvement of voltage-gated sodium channels (Na_v) that are essential for muscle excitability characteristics and for the acquisition of a mature phenotype[39]. We cannot exclude, however, a small contribution by calcium channels.

We next examined outward current densities measured at the end of the test pulse in WT and DYS cells at the same time points. As shown in the IV curves in Figure 5A and B, outward current density increased along the differentiation in both WT and DYS cells (Table 2), whereas D6 and D11 DYS cells present slightly higher (albeit not significant; Supporting Table S1) outward current densities compared to those of WT cells at the same days of differentiation (+60mV, Figure 5A, C; Table 2).

Barium-sensitive K^+ currents, such as currents carried by inward rectifier K^+ channels (Kir), are known to be expressed in fusion-competent myoblasts and especially in myocytes/myotubes where they contribute to hyperpolarization of the RMP [40]. Thus, to select barium-sensitive outward currents, 500 µM $BaCl_2$ was applied to the recording chamber. $BaCl_2$ decreased outward current densities in D11 WT cells by 67% but barely affected the outward component in D11 DYS cells (Figure 5D), suggesting the contribution of barium-insensitive channels to the outward component in differentiating myotubes, especially in DYS conditions.

Ion channel gene expression in WT and DYS myoblasts/myocytes

To support the electrophysiological data, we performed RT-PCR analysis of different ion channel genes that were possibly related to the recorded inward and outward currents. In particular, since both $Na_v1.4$ and $Na_v1.5$ can contribute to the inward current component, we analyzed the expression profile of their related genes *Scn4a* and *Scn5a*, respectively. Similarly, the outward component could be sustained by inwardly and delayed rectifying potassium channels and ClC-1 chloride channels. Thus, we measured the expression of *Kcnj2*, the gene encoding for Ba^{2+}-sensitive Kir2.1 channels, and of *Kcnq4* and *Kcna5* encoding for $K_v7.4$ and $K_v1.5$ channels, respectively, which are known to be expressed in skeletal muscle and be involved in myogenesis [41–43].We also monitored the expression of the *Clcn1* gene encoding for the skeletal muscle chloride channel ClC-

1, which is important for the stabilization of RMP and for the acquisition of more differentiated features[44].

In WT and DYS cells, *Scn4a* and *Scn5a* expression increased as differentiation proceeded (Figure 6A and B). However, *Scn4a* expression was expressed more in D11 WT compared with D11 DYS (Figure 6A; Supporting Table S1). Conversely, the expression of *Scn5a* was 5-fold higher in D11 DYS cells compared to WT cells (Figure 6B; Supporting Table 1). Moreover, no expression of *Scn4a* was found in D2 or D4 WT cells and D6 DYS cells. We did not find expression of *Scn5a* in D4 DYS cells. In addition, comparing the combined expression of *Scn4a* and *Scn5a* genes in stacked histograms, D11 DYS myocytes presented a smaller relative normalized expression of *Scn4a* than *Scn5a* with respect to D11 WT cells (Figure 6C). Immunofluorescence experiments supported the presence of $Na_v1.4$ and $Na_v1.5$ in both cell lines (Figure 7). Regarding ClC-1, *Clcn1* expression increased from D4 to D11 in WT cells (Figure 6D) but, interestingly, it was never found in DYS cells at any time points. *Kcnj2* expression level was very small in both cell types; however, it appeared to be significantly higher in D0, D4, and D11 DYS cells compared with WT myocytes (Figure 8A; Supporting Table S1), but significantly lower in D2 and D6. Furthermore, immunostaining of Kir2.1 channel confirmed the presence of the protein in both cell lines (Figure 8D). *Kcnq4* expression levels were similar in both D6 and D11 WT and DYS cells but was found to be higher in D2 and D4 DYS cells, compared to the same time points in WT myocytes (Figure 8B; Supporting Table S1). No *Kcnq4* was found in D0 DYS myoblasts. On the other hand, *Kcna5* expression was only present in D2 and D11 WT cells and increased as differentiation progressed (Figure 8C). Finally, we also looked for *Kcnj11* gene expression; however it was present in neither WT nor DYS cells (data not shown).

DISCUSSION

Myogenesis is a key process for skeletal muscle regeneration in adults and has been found to be altered in DMD settings [14,45]. Different ion channels interact with the DGC [12,22–25] and are known to contribute to muscle function during plasticity and disease [46,47]. Thus, in the complex scenario of DMD, the expression and activity of muscle specific ion channels can represent useful biomarkers to monitor myofiber differentiation state and appealing drug targets.

In this study we sought to evaluate the correlation between ion channel development during differentiation and how it could parallel the myogenic program in DMD settings by using WT and DYS myoblasts and differentiated muscle cells. We reported changes in membrane electrical properties and in ionic currents as well as in the expression of genes encoding for ion channels and regulators of myogenesis. These changes are suggestive of delayed differentiation in DYS cells compared to WT cells.

Myogenic transcription factors

Consistent with previously published data, the reduced expression of *Myog* and *Myf5* pointed to an impaired differentiation process in D6 and D11 DYS cells. The reduction of *Myog* could be due to the inefficacy of *Myf5*to support the myogenic program, as seen in satellite cells and myoblasts lacking both *Myf5*and *Myod* (both essential for the onset of myogenesis)[48]. In fact, fetal DMD muscles also show an overexpression of *PAX7* and reduced expression of *MYOD* (together with an alteration of calcium-mediated pathways)[49] . As discussed below, *Myog* reduction can also be a consequence of poor Kir2.1 expression in DYS cells[50] .

Inward and outward currents

The electrophysiological analysis revealed slight alterations in both inward and outward current components in DYS cells compared to WT. Our results show that, throughout differentiation, both WT and DYS cells have a significant increase of inward current densities from D0 to D11. However, DYS myocytes at D11 displayed slightly increased—but not significant—inward current density with respect to D11 WT cells. This increment, together with a smaller Cm, could imply an early stage sodium load already described in DMD settings [51].

The use of TTX corroborated the involvement of $Na_v1.4$ and $Na_v1.5$ channels in both cell lines, although we cannot exclude the possible contribution of calcium channels to the inward component. A clear difference between WT and DYS cell emerged from the analysis of sodium channel expression. $Na_v1.4$ (*SCN4A*) is the predominant sodium channel isoform in the adult skeletal muscle [51,52] whereas $Na_v1.5$ (*SCN5A*) is the most abundant sodium channel isoform in the heart, neonatal muscle, and after denervation [53,54]. Interestingly, D11 DYS cells showed a reduced total amount of *Scn4a* and *Scn5a* expression with a marked upregulation of *Scn5a* gene compared to control. Considering the time pattern of expression of *Scn5a*, its overexpression in DYS myocytes at D11 could be considered a sign of a delayed or impaired maturation in this cell line. These data would support previous findings showing that voltage gated sodium channels, essential for the excitability of skeletal muscle [55], can also play an important role in muscle cell differentiation and possibly in the myogenic process [56,57].

Importantly, $Na_v1.4$ channels, as well as $Na_v1.5$, are known to indirectly interact with dystrophin through the dystrophin-associated protein complex (DAPC). This suggests that the lack of dystrophin by disrupting this interaction[21] may alter its expression and functioning. In particular, different localization patterns and existence of macromolecular complexes have been described for $Na_v1.5$ channels in cardiomyocytes both at lateral membranes through the syntrophin–dystrophin

complex and at intercalated discs through SAP97[58,59]. Less information is available for $Na_v1.4$ localization in skeletal muscle fibers. Furthermore, the existence of different $Na_v1.4$-related macromolecular complexes has not been explored in detail nor whether changes in $Na_v1.4$ localization occurs in DMD muscles. Dedicated studies using specific tools to modulate $Na_v1.4$ channel expression would be useful to better understand the contribution of these and other ion channels in myogenesis in DMD cells. Furthermore, the importance of $Na_v1.4$ channels in myogenesis could be understood by investigating the consequences of $Na_v1.4$ dysfunction in mouse models or human diseases. For example, mice lacking $Na_v1.4$ do not survive beyond the second postnatal day[60] .

Both WT and DYS cell lines showed small outward current densities. Outward currents can be mediated by potassium ions outflow and/or to chloride ions influx; thus, we focused on barium-sensitive currents and on ClC-1 channels. Among barium-sensitive potassium channels, the key role of Kir2.1 in myoblast fusion has been described in cell cultures derived from human muscle biopsies [37,38,61]. Blockade of Kir2.1 channels in human WT myoblasts causes decreased or suppressed fusion and reduced expression of myogenic transcription factors.[47] In our murine derived cells, the expression of *Kcnj2* is small in both D11 WT and DYS cells. In addition, whereas the barium-sensitive component seemed to contribute only in part to the outward current in WT cells, DYS myocyte outward currents were almost barium-insensitive. In cardiomyocytes, a similar reduction of this Kir-mediated attribute has been observed in mdx ventricular cardiomyocytes [19] and in iPSC-cardiomyocytes from DMD patients [62.]

The lower expression of *Kcnj2* is also in agreement with reduced *Myog* mRNA level in DYS myocytes; this again corroborates that terminal differentiation may be altered in DYS cells. Of note, *Kcnj2* and *Myog* were overexpressed in D0 DYS cells compared to WT. This could suggest that myogenesis could also be altered in DYS myoblasts. Similar to $Na_v1.4$ and $Na_v1.5$, Kir2.1 is a member of the DAPC and binds to syntrophin[63]. Thus, again, dystrophin deficiency might impair

Kir2.1-mediated currents in skeletal muscle as proposed in the heart[64]. Furthermore, $Na_v1.5$ and Kir2.1 have been shown to traffic together to the sarcolemma of cardiomyocytes, creating macro-complexes and regulating both cardiac excitability and arrhythmogenesis [65,66]. Whether a mutual interaction occurs between $Na_v1.4$ and Kir2.1 channels, and perhaps other sarcolemmal channels, as well as the impact on skeletal muscle diseases and myogenesis is not known and would be worth exploring.

Besides Kir2.1, we explored the possible involvement of other potassium channels in myogenesis that may contribute to the outward currents in skeletal muscle cells, namely $K_v7.4$ and $K_v1.5$ [23,24,66]. In particular, our results show that the expression of the delayed rectifier $K_v7.4$ gene, *Kcnq4*, increased as differentiation progresses in WT cells, consistent with previously published data[67]. *Kcnq4* mRNA levels presented a similar increment in DYS cells, with an increase at D2 and D4, compared to WT cells at the same time points. The *Shaker* delayed rectifier potassium channel $K_v1.5$ acts principally during repolarization but is also involved in murine myoblast proliferation[41]. Interestingly, our results demonstrated that *Kcna5* expression increased along with differentiation in WT cells but was not present in DYS cells.

Remarkably, our RT-PCR showed a total absence of *Clcn1* mRNA in DYS cells at all time points and low expression in WT cells. ClC-1, the main chloride channel isoform in skeletal muscle, is the main actor responsible for the electrical stability of the sarcolemma. Its expression increases during muscle development and is controlled by innervation [68] and its activity varies depending on skeletal muscle pathophysiological conditions[69]. The lack of *Clcn1* in D11 DYS cells could be considered an early and indirect index of impaired myogenic potential. Despite the lack of evidence regarding the possible co-localization of the ClC-1 channel with DAPC, this finding corroborates the sensitivity of ClC-1 in the absence of dystrophin as hypothesized in adult myofibers of dystrophic mdx mice [70]. Specific direct recordings of ClC-1 channel current have always been

challenging in skeletal muscle[71–73] , and based on our results and current knowledge, we do not expect to see chloride currents in non-innervated myocytes.

RMP and Cm

Consistent with the lack of *Clcn1* and the smaller Kir-related current component in DYS myocytes, the RMP was more depolarized in DYS cells. Both Kir2.1 and ClC-1 channels contribute to setting resting membrane stability in skeletal muscle cells, and skeletal muscle fibers from mouse or humans carrying dysfunctional Kir2.1 or ClC-1 present changes in membrane potential and altered excitability [31,74]. The less negative RMP found in DYS cells could be associated to ~~a~~ cells less committed to the myogenic program ~~"immature" cell stage~~, In fact, RMP could be considered an indirect index of differentiation in fusion-competent myoblasts [30]. Importantly, a more depolarized RMP, if maintained throughout differentiation, affects the amount of Na_v channels in the resting state. It favors the non-conductive, inactivated state that has a clear impact on the ability to trigger a proper excitation–contraction coupling upon depolarization, which is also important to favor mechanically-stimulated differentiation. It should also be noted that the volume-regulated anion channel (VRAC or LRCC8) is another ion channel that can help myoblast differentiation by contributing to membrane hyperpolarization.[75–78]

Cm of D11 DYS cells was significantly lower than D6 DYS and D11 WT cells. This again suggests that DYS cells tend to get smaller, probably as a result of changes in membrane protein localization, possible lipid composition, epigenetic mechanisms, and/or delayed differentiation[29]. This would be consistent with a membrane less stable and more prone to damage due to the absence of dystrophin [79,75] Few authors have measured Cm in WT and DYS cells/fibers and there is no consensus on the relative Cm changes. Canato et al. found that mdx fibers present a lower Cm with respect to control mice values; similar results have been obtained in epicardial myocytes of adult

mdx dogs compared to age-matched control [80,81]. Conversely, Rivet and colleagues showed that Cm of human DMD myotubes was higher than controls [82].

CONCLUSIONS

Overall, the greater expression of *Scn5a,* the reduced barium sensitive outward currents, the absence of ClC-1, the smaller Cm and more depolarized RMP, together with reduced *Myog* and *Myf5* expression at different myocyte differentiation stages, all support a parallel defect in myogenic efficiency and acquired differentiated biophysical features compared to WT. The impairment of proper ion channel expression/function may in turn affect myogenesis in a sort of auto-reinforcing loop, eventually leading to what appears as dysfunctional regeneration.

Despite promising therapeutics in the pipeline, DMD still suffers from unmet clinical needs. Our electrophysiological characterization suggests that ion channels could be involved in the myogenic program and can be considered as biomarkers of myogenesis. Thus, understanding the altered pattern of ion channel development in DMD settings could be pivotal to shed further light on DMD pathophysiology and to pave a way for new pharmacological targets to enhance myogenesis and regeneration. Moreover, exploring differentiation even further (beyond day 11) could be pivotal to better understand ion channels' role in later stages of myogenesis. Finally, identification of specific ion channels that could be involved in the myogenic program both in healthy and DMD conditions could be useful for creating 3D platforms, such as muscle organoids.

We are aware that this is a preliminary characterization of ion channels in DYS skeletal muscle cells and more detailed experiments that use more specific solutions and voltage-step protocols as well as selective blockers or small RNA interference are required to confirm the role of

specific ion channels as biomarkers of differentiation in this pathological setting. Further studies are also needed to fully understand ion channel localization and interactions in DMD settings.

ACKNOWLEDGEMENTS

This work was supported by Fondazione per il Sud **(**BTS grant 2018-PDR-00351) and by #NEXTGENERATIONEU (NGEU) and funded by the Ministry of University and Research (MUR), National Recovery and Resilience Plan (NRRP), project MNESYS (PE0000006)—A Multiscale Integrated Approach to the Study of the Nervous System in Health and Disease (DN. 1553 11.10.2022). The research has also been supported by the funding initiative Horizon Europe Seeds 2021 (Next Generation EU-MUR D.M. 737/2021) for the project "Optogenetics for the development of organs-on-chips: new platforms for the study of advanced therapies in rare neuromuscular and oncological disorders", and the fellowship to Erika Caputo, in particular.

DATA AVAILABILITY STATEMENT

Data will be made available upon request.

AUTHOR CONTRIBUTIONS

A.D.L. conceived the original idea. A.G.C., A.D.L., P.I., and O.C. wrote the paper. D.W. and O.C. contributed to establishing the cell model. A.G.C. carried out electrophysiological experiments. A.G.C., B.B., R.Q., E. Cristiano, and E. Caputo contributed to RT-PCR and immunofluorescence experiments. A.G.C. and P.I. created figures and table. A.D.L., P.I., D.W., and P.I. reviewed and edited the text. All authors read and agreed to the published version of the manuscript.

COMPETING INTERESTS

The authors declare that they have no known competing financial interests or personal relationships that could have appeared to influence the work reported in this paper.

REFERENCES

1. Cossu G, Biressi S. Satellite cells, myoblasts and other occasional myogenic progenitors: possible origin, phenotypic features and role in muscle regeneration. *Seminars in cell & developmental biology*. 2005;16(4-5):623-631. doi:10.1016/j.semcdb.2005.07.003

2. Tajbakhsh S. Skeletal muscle stem cells in developmental versus regenerative myogenesis. *Journal of Internal Medicine*. 2009;266(4):372-389. doi:https://doi.org/10.1111/j.1365-2796.2009.02158.x

3. Bentzinger CF, Wang YX, Rudnicki MA. Building muscle: molecular regulation of myogenesis. *Cold Spring Harbor perspectives in biology*. 2012;4(2).

doi:10.1101/cshperspect.a008342

4. Shin M-K, Bang JS, Lee JE, et al. Generation of Skeletal Muscle Organoids from Human Pluripotent Stem Cells to Model Myogenesis and Muscle Regeneration. *International journal of molecular sciences*. 2022;23(9). doi:10.3390/ijms23095108

5. Jalal S, Dastidar S, Tedesco FS. Advanced models of human skeletal muscle differentiation, development and disease: Three-dimensional cultures, organoids and beyond. *Current Opinion in Cell Biology*. 2021;73:92-104. doi:https://doi.org/10.1016/j.ceb.2021.06.004

6. Omairi S, Hau K-L, Collins-Hooper H, et al. Regulation of the dystrophin-associated glycoprotein complex composition by the metabolic properties of muscle fibres. *Scientific Reports*. 2019;9(1):2770. doi:10.1038/s41598-019-39532-4

7. Wilson DGS, Tinker A, Iskratsch T. The role of the dystrophin glycoprotein complex in muscle cell mechanotransduction. *Communications Biology*. 2022;5(1):1022. doi:10.1038/s42003-022-03980-y

8. Yeung EW, Whitehead NP, Suchyna TM, Gottlieb PA, Sachs F, Allen DG. Effects of stretch-activated channel blockers on [Ca2+]i and muscle damage in the mdx mouse. *The Journal of physiology*. 2005;562(Pt 2):367-380. doi:10.1113/jphysiol.2004.075275

9. Fraysse B, Liantonio A, Cetrone M, et al. The alteration of calcium homeostasis in adult dystrophic mdx muscle fibers is worsened by a chronic exercise in vivo. *Neurobiology of disease*. 2004;17(2):144-154. doi:10.1016/j.nbd.2004.06.002

10. Kumar A, Khandelwal N, Malya R, Reid MB, Boriek AM. Loss of dystrophin causes aberrant mechanotransduction in skeletal muscle fibers. *FASEB journal : official publication of the Federation of American Societies for Experimental Biology*. 2004;18(1):102-113.

doi:10.1096/fj.03-0453com

11. Mouly V, Aamiri A, Bigot A, et al. The mitotic clock in skeletal muscle regeneration, disease and cell mediated gene therapy. *Acta physiologica Scandinavica*. 2005;184(1):3-15. doi:10.1111/j.1365-201X.2005.01417.x

12. Leyva-Leyva M, Sandoval A, Felix R, González-Ramírez R. Biochemical and Functional Interplay Between Ion Channels and the Components of the Dystrophin-Associated Glycoprotein Complex. *The Journal of membrane biology*. 2018;251(4):535-550. doi:10.1007/s00232-018-0036-9

13. Cappellari O, Mantuano P, De Luca A. "The Social Network" and Muscular Dystrophies: The Lesson Learnt about the Niche Environment as a Target for Therapeutic Strategies. *Cells*. 2020;9(7). doi:10.3390/cells9071659

14. Dumont NA, Wang YX, von Maltzahn J, et al. Dystrophin expression in muscle stem cells regulates their polarity and asymmetric division. *Nature medicine*. 2015;21(12):1455-1463. doi:10.1038/nm.3990

15. Choi JH, Jeong SY, Oh MR, Allen PD, Lee EH. TRPCs: Influential Mediators in Skeletal Muscle. *Cells*. 2020;9(4). doi:10.3390/cells9040850

16. Pedersen TH, Riisager A, de Paoli FV, Chen T-Y, Nielsen OB. Role of physiological ClC-1 Cl- ion channel regulation for the excitability and function of working skeletal muscle. *The Journal of general physiology*. 2016;147(4):291-308. doi:10.1085/jgp.201611582

17. Hinard V, Belin D, Konig S, Bader CR, Bernheim L. Initiation of human myoblast differentiation via dephosphorylation of Kir2.1 K+ channels at tyrosine 242. *Development*. 2008;135(5):859-867. doi:10.1242/dev.011387

18. Kurosaka M, Ogura Y, Funabashi T, Akema T. Involvement of Transient Receptor Potential Cation Channel Vanilloid 1 (TRPV1) in Myoblast Fusion. *Journal of cellular physiology*. 2016;231(10):2275-2285. doi:10.1002/jcp.25345

19. Rubi L, Koenig X, Kubista H, Todt H, Hilber K. Decreased inward rectifier potassium current I(K1) in dystrophin-deficient ventricular cardiomyocytes. *Channels (Austin, Tex)*. 2017;11(2):101-108. doi:10.1080/19336950.2016.1228498

20. Bijlenga P, Liu JH, Espinos E, et al. T-type alpha 1H Ca2+ channels are involved in Ca2+ signaling during terminal differentiation (fusion) of human myoblasts. *Proceedings of the National Academy of Sciences of the United States of America*. 2000;97(13):7627-7632. doi:10.1073/pnas.97.13.7627

21. Constantin B. Dystrophin complex functions as a scaffold for signalling proteins. *Biochimica et biophysica acta*. 2014;1838(2):635-642. doi:10.1016/j.bbamem.2013.08.023

22. Gee SH, Madhavan R, Levinson SR, Caldwell JH, Sealock R, Froehner SC. Interaction of muscle and brain sodium channels with multiple members of the syntrophin family of dystrophin-associated proteins. *The Journal of neuroscience : the official journal of the Society for Neuroscience*. 1998;18(1):128-137. doi:10.1523/JNEUROSCI.18-01-00128.1998

23. Friedrich O, von Wegner F, Chamberlain JS, Fink RHA, Rohrbach P. L-type Ca2+ channel function is linked to dystrophin expression in mammalian muscle. *PloS one*. 2008;3(3):e1762. doi:10.1371/journal.pone.0001762

24. Sabourin J, Lamiche C, Vandebrouck A, et al. Regulation of TRPC1 and TRPC4 cation channels requires an alpha1-syntrophin-dependent complex in skeletal mouse myotubes. *The Journal of biological chemistry*. 2009;284(52):36248-36261. doi:10.1074/jbc.M109.012872

25. Leonoudakis D, Conti LR, Anderson S, et al. Protein trafficking and anchoring complexes revealed by proteomic analysis of inward rectifier potassium channel (Kir2.x)-associated proteins. *The Journal of biological chemistry*. 2004;279(21):22331-22346. doi:10.1074/jbc.M400285200

26. Adams ME, Mueller HA, Froehner SC. In vivo requirement of the alpha-syntrophin PDZ domain for the sarcolemmal localization of nNOS and aquaporin-4. *The Journal of cell biology*. 2001;155(1):113-122. doi:10.1083/jcb.200106158

27. Muses S, Morgan JE, Wells DJ. A New Extensively Characterised Conditionally Immortal Muscle Cell-Line for Investigating Therapeutic Strategies in Muscular Dystrophies. *PLOS ONE*. 2011;6(9):e24826. https://doi.org/10.1371/journal.pone.0024826

28. Muses S, Morgan JE, Wells DJ. Restoration of dystrophin expression using the Sleeping Beauty transposon. *PLoS currents*. 2011;3:RRN1296. doi:10.1371/currents.RRN1296

29. Boccanegra B, Mantuano P, Conte E, et al. LKB1 signaling is altered in skeletal muscle of a Duchenne muscular dystrophy mouse model. *Disease Models & Mechanisms*. 2023;16(7):dmm049930. doi:10.1242/dmm.049930

30. Guarnieri S, Morabito C, Belia S, et al. New Insights into the Relationship between mIGF-1-Induced Hypertrophy and Ca2+ Handling in Differentiated Satellite Cells. *PLOS ONE*. 2014;9(9):e107753. https://doi.org/10.1371/journal.pone.0107753

31. Sacconi S, Simkin D, Arrighi N, et al. Mechanisms underlying Andersen's syndrome pathology in skeletal muscle are revealed in human myotubes. *American Journal of Physiology-Cell Physiology*. 2009;297(4):C876-C885. doi:10.1152/ajpcell.00519.2008

32. Boccanegra B, Cappellari O, Mantuano P, et al. Growth hormone secretagogues modulate

inflammation and fibrosis in mdx mouse model of Duchenne muscular dystrophy . *Frontiers in Immunology* . 2023;14. https://www.frontiersin.org/articles/10.3389/fimmu.2023.1119888

33. Pownall ME, Gustafsson MK, Emerson CPJ. Myogenic regulatory factors and the specification of muscle progenitors in vertebrate embryos. *Annual review of cell and developmental biology*. 2002;18:747-783. doi:10.1146/annurev.cellbio.18.012502.105758

34. Hildyard JCW, Wells DJ. Identification and validation of quantitative PCR reference genes suitable for normalizing expression in normal and dystrophic cell culture models of myogenesis. *PLoS currents*. 2014;6. doi:10.1371/currents.md.faafdde4bea8df4aa7d06cd5553119a6

35. Golowasch J, Nadim F. Capacitance, Membrane BT - Encyclopedia of Computational Neuroscience. In: Jaeger D, Jung R, eds. Springer New York; 2014:1-5. doi:10.1007/978-1-4614-7320-6_32-1

36. Fioretti B, Pietrangelo T, Catacuzzeno L, Franciolini F. Intermediate-conductance Ca2+-activated K+ channel is expressed in C2C12 myoblasts and is downregulated during myogenesis. *American Journal of Physiology-Cell Physiology*. 2005;289(1):C89-C96. doi:10.1152/ajpcell.00369.2004

37. Fischer-Lougheed J, Liu JH, Espinos E, et al. Human myoblast fusion requires expression of functional inward rectifier Kir2.1 channels. *The Journal of cell biology*. 2001;153(4):677-686. doi:10.1083/jcb.153.4.677

38. Bijlenga P, Occhiodoro T, Liu JH, Bader CR, Bernheim L, Fischer-Lougheed J. An ether -à-go-go K+ current, Ih-eag, contributes to the hyperpolarization of human fusion-competent myoblasts. *The Journal of physiology*. 1998;512 (Pt 2(Pt 2):317-323. doi:10.1111/j.1469-

7793.1998.317be.x

39. Morel J, Rannou F, Talarmin H, et al. Sodium channel Na(V)1.5 expression is enhanced in cultured adult rat skeletal muscle fibers. *The Journal of membrane biology*. 2010;235(2):109-119. doi:10.1007/s00232-010-9262-5

40. Konig S, Hinard V, Arnaudeau S, et al. Membrane hyperpolarization triggers myogenin and myocyte enhancer factor-2 expression during human myoblast differentiation. *Journal of Biological Chemistry*. 2004;279(27):28187-28196. doi:10.1074/jbc.M313932200

41. Villalonga N, Martínez-Mármol R, Roura-Ferrer M, et al. Cell cycle-dependent expression of Kv1.5 is involved in myoblast proliferation. *Biochimica et biophysica acta*. 2008;1783(5):728-736. doi:10.1016/j.bbamcr.2008.01.001

42. Iannotti FA, Barrese V, Formisano L, Miceli F, Taglialatela M. Specification of skeletal muscle differentiation by repressor element-1 silencing transcription factor (REST)-regulated Kv7.4 potassium channels. *Molecular biology of the cell*. 2013;24(3):274-284. doi:10.1091/mbc.E11-12-1044

43. Roura-Ferrer M, Solé L, Martínez-Mármol R, Villalonga N, Felipe A. Skeletal muscle Kv7 (KCNQ) channels in myoblast differentiation and proliferation. *Biochemical and biophysical research communications*. 2008;369(4):1094-1097. doi:10.1016/j.bbrc.2008.02.152

44. Bardouille C, Vullhorst D, Jockusch H. Expression of chloride channel 1 mRNA in cultured myogenic cells: a marker of myotube maturation. *FEBS letters*. 1996;396(2-3):177-180. doi:10.1016/0014-5793(96)01098-8

45. Delaporte C, Dehaupas M, Fardeau M. Comparison between the growth pattern of cell cultures from normal and Duchenne dystrophy muscle. *Journal of the neurological sciences*.

1984;64(2):149-160. doi:10.1016/0022-510x(84)90033-9

46. Pierno S, Desaphy J-F, Liantonio A, et al. Change of chloride ion channel conductance is an early event of slow-to-fast fibre type transition during unloading-induced muscle disuse. *Brain : a journal of neurology*. 2002;125(Pt 7):1510-1521. doi:10.1093/brain/awf162

47. Desaphy J-F, De Luca A, Imbrici P, Conte Camerino D. Modification by ageing of the tetrodotoxin-sensitive sodium channels in rat skeletal muscle fibres. *Biochimica et Biophysica Acta (BBA) - Biomembranes*. 1998;1373(1):37-46. doi:https://doi.org/10.1016/S0005-2736(98)00085-6

48. Yamamoto M, Legendre NP, Biswas AA, et al. Loss of MyoD and Myf5 in Skeletal Muscle Stem Cells Results in Altered Myogenic Programming and Failed Regeneration. *Stem cell reports*. 2018;10(3):956-969. doi:10.1016/j.stemcr.2018.01.027

49. Farini A, Sitzia C, Cassinelli L, et al. Inositol 1,4,5-trisphosphate (IP3)-dependent Ca2+ signaling mediates delayed myogenesis in Duchenne muscular dystrophy fetal muscle. *Development*. 2016;143(4):658-669. doi:10.1242/dev.126193

50. Konig S, Hinard V, Arnaudeau S, et al. Membrane hyperpolarization triggers myogenin and myocyte enhancer factor-2 expression during human myoblast differentiation. *The Journal of biological chemistry*. 2004;279(27):28187-28196. doi:10.1074/jbc.M313932200

51. Hirn C, Shapovalov G, Petermann O, Roulet E, Ruegg UT. Nav1.4 deregulation in dystrophic skeletal muscle leads to Na+ overload and enhanced cell death. *The Journal of general physiology*. 2008;132(2):199-208. doi:10.1085/jgp.200810024

52. Teener JW, Rich MM. Dysregulation of sodium channel gating in critical illness myopathy. *Journal of muscle research and cell motility*. 2006;27(5-7):291-296. doi:10.1007/s10974-

006-9074-5

53. Balser JR. The cardiac sodium channel: gating function and molecular pharmacology. *Journal of molecular and cellular cardiology*. 2001;33(4):599-613. doi:10.1006/jmcc.2000.1346

54. Kallen RG, Sheng ZH, Yang J, Chen LQ, Rogart RB, Barchi RL. Primary structure and expression of a sodium channel characteristic of denervated and immature rat skeletal muscle. *Neuron*. 1990;4(2):233-242. doi:10.1016/0896-6273(90)90098-z

55. Ruff RL. Sodium channel regulation of skeletal muscle membrane excitability. *Annals of the New York Academy of Sciences*. 1997;835:64-76. doi:10.1111/j.1749-6632.1997.tb48618.x

56. David M, Martínez-Mármol R, Gonzalez T, Felipe A, Valenzuela C. Differential regulation of Na(v)beta subunits during myogenesis. *Biochemical and biophysical research communications*. 2008;368(3):761-766. doi:10.1016/j.bbrc.2008.01.138

57. Chen L, Hassani Nia F, Stauber T. Ion Channels and Transporters in Muscle Cell Differentiation. *International Journal of Molecular Sciences* . 2021;22(24). doi:10.3390/ijms222413615

58. Petitprez S, Zmoos A-F, Ogrodnik J, et al. SAP97 and dystrophin macromolecular complexes determine two pools of cardiac sodium channels Nav1.5 in cardiomyocytes. *Circulation research*. 2011;108(3):294-304. doi:10.1161/CIRCRESAHA.110.228312

59. Abriel H, Rougier J-S, Jalife J. Ion channel macromolecular complexes in cardiomyocytes: roles in sudden cardiac death. *Circulation research*. 2015;116(12):1971-1988. doi:10.1161/CIRCRESAHA.116.305017

60. Wu F, Mi W, Fu Y, Struyk A, Cannon SC. Mice with an NaV1.4 sodium channel null allele

have latent myasthenia, without susceptibility to periodic paralysis. *Brain : a journal of neurology*. 2016;139(Pt 6):1688-1699. doi:10.1093/brain/aww070

61. Liu JH, Bijlenga P, Fischer-Lougheed J, et al. Role of an inward rectifier K+ current and of hyperpolarization in human myoblast fusion. *The Journal of physiology*. 1998;510 (Pt 2(Pt 2):467-476. doi:10.1111/j.1469-7793.1998.467bk.x

62. Jimenez-Vazquez EN, Arad M, Macías Á, et al. SNTA1 gene rescues ion channel function and is antiarrhythmic in cardiomyocytes derived from induced pluripotent stem cells from muscular dystrophy patients. Huang CL-H, Barton M, Huang CL-H, eds. *eLife*. 2022;11:e76576. doi:10.7554/eLife.76576

63. Koenig X, Ebner J, Hilber K. Voltage-Dependent Sarcolemmal Ion Channel Abnormalities in the Dystrophin-Deficient Heart. *International journal of molecular sciences*. 2018;19(11). doi:10.3390/ijms19113296

64. Allen DG, Whitehead NP, Froehner SC. Absence of Dystrophin Disrupts Skeletal Muscle Signaling: Roles of Ca2+, Reactive Oxygen Species, and Nitric Oxide in the Development of Muscular Dystrophy. *Physiological reviews*. 2016;96(1):253-305. doi:10.1152/physrev.00007.2015

65. Willis BC, Ponce-Balbuena D, Jalife J. Protein assemblies of sodium and inward rectifier potassium channels control cardiac excitability and arrhythmogenesis. *American journal of physiology Heart and circulatory physiology*. 2015;308(12):H1463-73. doi:10.1152/ajpheart.00176.2015

66. Ponce-Balbuena D, Guerrero-Serna G, Valdivia CR, et al. Cardiac Kir2.1 and Na(V)1.5 Channels Traffic Together to the Sarcolemma to Control Excitability. *Circulation research*. 2018;122(11):1501-1516. doi:10.1161/CIRCRESAHA.117.311872

67. Iannotti FA, Panza E, Barrese V, Viggiano D, Soldovieri MV, Taglialatela M. Expression, localization, and pharmacological role of Kv7 potassium channels in skeletal muscle proliferation, differentiation, and survival after myotoxic insults. *The Journal of pharmacology and experimental therapeutics*. 2010;332(3):811-820. doi:10.1124/jpet.109.162800

68. De Luca A, Mambrini M, Conte Camerino D. Changes in membrane ionic conductances and excitability characteristics of rat skeletal muscle during aging. *Pflügers Archiv*. 1990;415(5):642-644. doi:10.1007/BF02583519

69. Altamura C, Desaphy J-F, Conte D, De Luca A, Imbrici P. Skeletal muscle ClC-1 chloride channels in health and diseases. *Pflugers Archiv : European journal of physiology*. 2020;472(7):961-975. doi:10.1007/s00424-020-02376-3

70. De Luca A, Pierno S, Liantonio A, et al. Alteration of excitation-contraction coupling mechanism in extensor digitorum longus muscle fibres of dystrophic mdx mouse and potential efficacy of taurine. *British journal of pharmacology*. 2001;132(5):1047-1054. doi:10.1038/sj.bjp.0703907

71. De Luca A, Pierno S, Camerino DC. Effect of taurine depletion on excitation-contraction coupling and Cl- conductance of rat skeletal muscle. *European journal of pharmacology*. 1996;296(2):215-222. doi:10.1016/0014-2999(95)00702-4

72. Leermakers PA, Dybdahl KLT, Husted KS, et al. Depletion of ATP Limits Membrane Excitability of Skeletal Muscle by Increasing Both ClC1-Open Probability and Membrane Conductance . *Frontiers in Neurology* . 2020;11. https://www.frontiersin.org/articles/10.3389/fneur.2020.00541

73. Cozzoli A, Liantonio A, Conte E, et al. Angiotensin II modulates mouse skeletal muscle

resting conductance to chloride and potassium ions and calcium homeostasis via the AT1 receptor and NADPH oxidase. *American journal of physiology Cell physiology*. 2014;307(7):C634-47. doi:10.1152/ajpcell.00372.2013

74. Mehrke G, Brinkmeier H, Jockusch H. The myotonic mouse mutant ADR: electrophysiology of the muscle fiber. *Muscle & nerve*. 1988;11(5):440-446. doi:10.1002/mus.880110505

75. Chen L, König B, Stauber T. LRRC8 channel activation and reduction in cytosolic chloride concentration during early differentiation of C2C12 myoblasts. *Biochemical and biophysical research communications*. 2020;532(3):482-488. doi:10.1016/j.bbrc.2020.08.080

76. Voets T, Droogmans G, Nilius B. Modulation of voltage-dependent properties of a swelling-activated Cl- current. *The Journal of general physiology*. 1997;110(3):313-325. doi:10.1085/jgp.110.3.313

77. Kumar A, Xie L, Ta CM, et al. SWELL1 regulates skeletal muscle cell size, intracellular signaling, adiposity and glucose metabolism. *eLife*. 2020;9. doi:10.7554/eLife.58941

78. Chen L, Becker TM, Koch U, Stauber T. The LRRC8/VRAC anion channel facilitates myogenic differentiation of murine myoblasts by promoting membrane hyperpolarization. *The Journal of biological chemistry*. 2019;294(39):14279-14288. doi:10.1074/jbc.RA119.008840

79. Petrof BJ, Shrager JB, Stedman HH, Kelly AM, Sweeney HL. Dystrophin protects the sarcolemma from stresses developed during muscle contraction. *Proceedings of the National Academy of Sciences of the United States of America*. 1993;90(8):3710-3714. doi:10.1073/pnas.90.8.3710

80. Canato M, Dal Maschio M, Sbrana F, et al. Mechanical and electrophysiological properties

of the sarcolemma of muscle fibers in two murine models of muscle dystrophy: col6a1-/- and mdx. *Journal of biomedicine & biotechnology*. 2010;2010:981945. doi:10.1155/2010/981945

81. Pacioretty LM, Cooper BJ, Gilmour RF. Reduction of the transient outward potassium current in canine X-linked muscular dystrophy. *Circulation*. 1994;90(3):1350-1356. doi:10.1161/01.CIR.90.3.1350

82. Rivet M, Cognard C, Rideau Y, Duport G, Raymond G. Calcium currents in normal and dystrophic human skeletal muscle cells in culture. *Cell calcium*. 1990;11(8):507-514. doi:10.1016/0143-4160(90)90026-q

FIGURE LEGENDS

FIGURE 1 Bright-field images depicting WT and DYS myoblasts and D11 myocytes. Myoblasts (red arrows) have a rounder shape than myotubes and present spindles (blue arrows), whereas myotubes (yellow arrows) show a more elongated form than muscle cells in proliferation. Scale bars: 100 µm. Abbreviations: D0, myoblasts; D11, Day 11; DYS, dystrophic; WT, wild-type.

FIGURE 2 Gene expression (relative to zero) of different markers of differentiation/myogenesis in WT and DYS myoblasts (D0), and myocytes (D2–D11). (A) *Myf5*, (B) myogenin (*Myog*) and (C) dystrophin gene (*Dmd*). For some time points mRNA expression was barely detectable. Student's t test *$p \leq 0.05$, ** $p \leq 0.01$, *** $p \leq 0.001$, **** $p \leq 0.0001$. (D) Immunostaining of dystrophin (red), phalloidin (green) and nuclei (blue) in D11 WT and DYS cells. Last panel on the right, Red,

Green, Blue (RGB) merged image. Scale bars: 100 µm.

FIGURE 3 (A) Membrane capacitance and (B) resting membrane potential in WT and DYS myoblasts and D2–D11 myocytes. (A) Shows significant differences between the two cell lines during differentiation. Data are mean ± S.E.M of the indicated number of cells. Student's t test * $p \leq 0.001$, *** $p \leq 0.001$. Abbreviations: DYS, dystrophic; WT, wild-type.

Table 2. Total inward and outward current density measured at -20 mV and at +60 mV, respectively, at D0 (myoblasts) and D2-D11 (myocytes). Cm and RMP values from D0 to D11. TTX and $BaCl_2$ effect is recorded at D6/11 in WT/DYS myocytes. Data are mean ± S.E.M of the indicated number of cells (n). The number of cell batches (N) from which we recorded different cells n is also indicated. Student's t test: *$p \leq 0.05$, *** $p \leq 0.001$. Abbreviations: DYS, dystrophic; TTX, tetrodotoxin; WT, wild-type.; Cm, Capacitance; Resting membrane potential (RMP).

FIGURE 4 Inward current density in WT and DYS myoblasts and myocytes. IV curves of (A) WT and (B) DYS myoblasts (D0) and myocytes (D2–D11). Insets show inward currents in WT and DYS myocytes. (C) Bar graph showing the inward current density (at -20 mV) of WT and DYS myoblasts and D2–D11 myocytes;. A statistically significant difference was found only for inward current densities within WT cells at all time points. One-way ANOVA for WT ($p \leq 0.01$) and DYS ($p=0.087$) (Supporting Table S2). (D) Bar graph showing the effect of TTX in WT and DYS at D6 and D11. Data are mean ± S.E.M of the indicated *n* of cells Abbreviations: DYS, dystrophic; TTX,

tetrodotoxin; WT, wild-type.

FIGURE 5 Outward current density in WT and DYS myoblasts and myocytes. IV curves of (A) WT and (B) DYS myoblasts (D0) and myocytes (D2–D11). Insets show the outward current component in WT and DYS myocytes; the inward component was cut from the traces for clarity reasons. (C) Bar graph showing the outward current density (at +60 mV) of WT and DYS myoblasts and D2–D11 myocytes. A statistically significant difference was found for outward current densities within WT and within DYS at all time points. One-way ANOVA for WT ($p \leq 0.0001$) and DYS ($p \leq 0.05$) (Supporting Table S2). (D) Bar graph showing the comparison of the effect of $BaCl_2$ in WT and DYS myocytes at D6 and D11. Data are mean ± S.E.M of the indicated *n* of cells. Abbreviations: DYS, dystrophic; WT, wild-type.

FIGURE 6 Gene expression (relative to zero) of different ion channels in WT and DYS myoblasts (D0), and myocytes (D2–D11). (A) *Scn4a* gene for the Nav1.4. (B) *Scn5a* gene for the $Na_v1.5$. (C) Stacked histograms depicting *Scn4a* and *Scn5a* relative expression for each differentiation time point in both cell lines. (D) *Clcn1* gene for the skeletal muscle chloride channel, ClC-1. For some time points no mRNA expression was found. Student's t test *$p \leq 0.05$, ** $p \leq 0.01$, *** $p \leq 0.001$, **** $p \leq 0.0001$. Abbreviations: DYS, dystrophic; WT, wild-type.

FIGURE 7 Immunofluorescence of D11 WT and DYS cells. Cells were stained with DAPI for nuclei (Blue), polyclonal anti-sodium channel $Na_v1.4$ and $Na_v1.5$ (Green), MF20-S for myosin (Red). Last panel on the right, Red, Green, Blue (RGB) merged image. (A) D11 WT and (B) DYS cells stained with antibodies for $Na_v1.4$ and myosin; (C) WT and (D) DYS cells at D11 with

polyclonal anti-$Na_v1.5$ and monoclonal pan antibody against myosin. Scale bars: 100 µm. Abbreviations: DYS, dystrophic; WT, wild-type.

FIGURE 8 Gene expression (relative to zero) of potassium ion channels in WT and DYS myoblasts (D0), and myocytes (D2–D11). (A) *Kcnj2* for inward rectifying Kir2.1 (B) *Kcnq4* voltage-gated channel $K_v7.4$ (C) *Kcna5* for voltage-gated channel $K_v1.5$. For some time points no mRNA expression was detected. Student's t test *$p \leq 0.05$, ** $p \leq 0.01$ *** $p \leq 0.001$ **** $p \leq 0.0001$. (D) Immunostaining of Kir2.1 (Green), myosin, and nuclei (Blue) in D11 WT and DYS cells. Last panel on the right, Red, Green, Blue (RGB) merged image. Scale bars: 100 µm. Abbreviations: DYS, dystrophic; WT, wild-type.